

Wettability characteristics of an $\text{Al}_2\text{O}_3/\text{SiO}_2$ based ceramic modified with CO_2 , Nd:YAG, excimer and high power diode lasers

J. Lawrence and L. Li

Manufacturing Division, Department of Mechanical Engineering, University of Manchester
Institute of Science and Technology (UMIST), Manchester, M60 1QD, UK.

Correspondence

Mr. Jonathan Lawrence / Dr. Lin Li
Manufacturing Division,
Department of Mechanical Engineering,
University of Manchester Institute of Science and Technology (UMIST),
Manchester,
M60-1QD,
UK.

Tel : (44) (44) 161 200-3816
Fax : (44) 161 200-3803
e-mail : J.Lawrence@stud.umist.ac.uk / L.Li@umist.ac.uk

Abstract

Interaction of CO₂, Nd:YAG, excimer and high power diode laser (HPDL) radiation with the surface of an Al₂O₃/SiO₂ based ceramic was found to effect significant changes in the wettability characteristics of the material. It was observed that interaction with CO₂, Nd:YAG and HPDL radiation reduced the enamel contact angle from 118° to 31°, 34° and 33° respectively. In contrast, interaction with excimer laser radiation resulted an increase in the contact angle to 121°. Such changes were identified as being due to: (i) the melting and partial vitrification of the Al₂O₃/SiO₂ based ceramic surface as a result of interaction with CO₂, Nd:YAG HPDL radiation. (ii) the surface roughness of the Al₂O₃/SiO₂ based ceramic increasing after interaction with excimer laser radiation. (iii) the surface oxygen content of the Al₂O₃/SiO₂ based ceramic increasing after interaction with CO₂, Nd:YAG and HPDL radiation. The work has shown that the wettability characteristics of the Al₂O₃/SiO₂ based ceramic could be controlled and/or modified with laser surface treatment. In particular, whether the laser radiation had the propensity to cause surface melting. However, a wavelength dependance of the change of the wetting properties could not be deduced from the findings of this work.

Keywords: CO₂ laser, Nd:YAG laser, excimer laser, high power diode laser (HPDL), surface energy, wettability, enamel, alumina, silica, ceramic

PACS: (2.55.P) (42.70.H) (68.45.G)

1. Introduction

Studies of the effects of laser wavelength variation for medical and surgical applications are numerous [1-7], and have shown clear differences in the performance and effectiveness of many different lasers for such applications. Comparisons of the differences in the beam interaction characteristics with various materials of the predominant materials processing lasers, the CO₂, the Nd:YAG and the excimer laser, are limited. Previously Dausinger [8] compared CO, CO₂ and Nd:YAG lasers for a number of materials processing applications, noting the main fundamental differences resulting from wavelength variations. From work using CO₂ and excimer lasers to examine the effect of laser wavelength on the ablation of soda-lime-silica glass, Shuttleworth [9] observed distinct differences in the performance of the lasers in terms of process effectiveness. Similarly, from work investigating alternative routes to the laser ablation-deposition (LAD) of Al₂O₃ and Ti:sapphire using CO₂ and excimer radiation, Dyer et al [10] found that laser wavelength was a major influence in determining the likelihood of successful deposition. A study conducted by Chen et al [11] using Nd:YAG and excimer lasers found that the quality of laser drilled holes was significantly influenced by laser wavelength.

Likewise such practical comparisons between these traditional materials processing lasers and the more contemporary high power diode laser (HPDL) are even fewer in number. Previously Schmidt et al [12] compared the performance of CO₂, excimer and HPDL in the removal of chlorinated rubber coatings from concrete surfaces, particularly in terms of removal rate. From the work, wavelength dependant differences in process performance were observed. Additionally, Bradley et al [13] compared the CO₂ and HPDL for the treatment of Al₂O₃-based refractory materials in terms of microstructure, observing wavelength dependant microstructural characteristics unique to each laser.

This paper reports on work conducted to determine the differences in the beam interaction characteristics of an Al₂O₃/SiO₂ based ceramic material and a commercially available vitreous enamel with a 1 kW CO₂ laser, a 400 W Nd:YAG laser, a 5 W KrF excimer laser and a 60 W-cw HPDL, with particular emphasis on the laser effected modification of the wettability characteristics.

Wetting is often the primary factor governing whether a coating will adhere and bond to a substrate in practical applications such as enamelling, painting, etc. In this present study the Al₂O₃/SiO₂ based ceramic used is a newly developed ceramic tile grout material (an amalgamated oxide compound grout (AOCG)), which in practice is sealed by firing the enamel

frit onto it using a HPDL, thus creating an impervious surface glaze [14-16]. As such, it is most important to understand the fundamental behaviour and the mechanisms involved in the laser firing of the enamel on to the AOCCG.

Both scientists and engineers alike have a great interest in understanding the interfacial phenomena between vitreous enamels and ceramic materials, since in many practical applications where vitreous enamels are fired onto ceramic substrates, the performance of the article is directly linked to the nature of the enamel-ceramic interface. At present, very little work has been published with regard to the use of lasers for altering the surface properties of materials in order to improve their wettability characteristics. Notwithstanding this, it is recognised within the currently published work that laser irradiation of material surfaces can effect its wettability characteristics. Previously Zhou et al [17, 18] have carried out work on laser coating of aluminium alloys with ceramic materials (SiO_2 , Al_2O_3 , etc.), reporting on the well documented fact that generated oxide layers often promote metal/oxide wetting. Bahners et al [19, 20], have observed and comprehensively detailed the changes in technical properties of various textile fibres, including adhesion and wetting properties, with a view to developing an alternative to the conventional methods of chemical agents addition or wet-chemical pre-processing. Also, Heitz et al [21] and Olfert et al [22] have found that excimer laser treatment of metals results in improved coating adhesion. The improvements in adhesion were ascribed to the fact that the excimer laser treatment resulted in a smoother surface and as such enhanced the action of wetting. However, the reasons for these changes with regard to changes in the material's surface morphology, surface composition and surface energy are not reported.

Work on HPDL modification of the wettability characteristics of a number of different ceramic materials [23] has shown that the wettability performance is affected by changes in the surface roughness, the surface O_2 content and the surface energy. This paper reports specifically on the interaction characteristics of the beams of all four lasers with the AOCCG and the enamel in terms of resultant changes in the wettability characteristics. These incorporate chiefly: contact angle variations, the differences in morphological features, the surface composition, the microstructural changes and the surface energy changes.

2. Experimental procedure

2.1. Material preparation and application procedure

The ceramic material consisted of mixed vitrifiable oxide powders such as chamotte (mainly SiO_2 (53wt%) and Al_2O_3 (42wt%)), Fe_2O_3 , MgO , ZrO_2 and ZnO was produced. The oxide powders were sieved to ensure a particle size of less than $75\mu\text{m}$, then thoroughly mixed

together to ensure homogeneity, along with approximately 50wt% diluted sodium silicate solution so as to form a manageable paste. The AOCG was then pasted on to an ordinary Portland cement (OPC) substrate to a thickness of 2mm and allowed to cure at room temperature for 12 hours. The composition of the enamel consisted mainly of the following; SiO_2 , B_2O_3 , Na_2O , Mn, F and small quantities of Ba, Al_2O_3 and Ni, whilst the powder size was less than $75\mu\text{m}$. The enamel frit paste was allowed to cure at room temperature for one to two hours and then irradiated immediately with the HPDL beam.

2.2. Laser processing procedures

Figure 1 schematically illustrates the general laser processing experimental arrangement, where the defocused beams of the lasers were fired back and forth across the surfaces of the AOCG by traversing the samples beneath the laser beam using the x- and y-axis of the CNC gantry table. The general operating characteristics of the lasers used in the study are detailed in Table1. Both pulsed and CW lasers were used in the study, therefore, both the average power and the peak power of each laser will differ. So, in order to reasonably compare the effects of each laser on the wettability characteristics of the AOCG, the laser energy density (fluence) of each laser beam incident on the AOCG surface was set by manipulating the laser power densities and traverse speeds such that the energy density of each of the four lasers incident upon the AOCG surface was around 165 J/cm^2 .

2.3. Contact angle and surface energy analysis procedure

To investigate the effects of laser radiation on the wetting and surface energy characteristics of the AOCG, two sets of wetting experiments were conducted. The first set of experiments were to simply determine the contact angle between the enamel and the AOCG before and after interaction with the selected industrial lasers. The second set of experiments were control experiments carried out using the sessile drop technique with a variety of test liquids with known surface energy properties in order to quantify any surface energy changes in the AOCG resulting from laser interaction.

The enamel-AOCG wetting experiments were carried out in atmospheric conditions with molten droplets of the enamel (600°C). The temperature of the enamel throughout the experiments was measured using a Cyclops infrared pyrometer. The droplets were released in a controlled manner onto the surface of the AOCG (laser treated and untreated) from the tip of a micropipette, with the resultant volume of the drops being approximately $15 \times 10^{-3} \text{ cm}^3$. Profile photographs of the sessile enamel drop were obtained for every 60°C fall in temperature of the molten enamel drop, with the contact angle subsequently being measured, and a mean value being obtained.

The sessile drop control experiments were carried out, using human blood, human blood plasma, glycerol and 4-octanol. The test liquids, along with their total surface energy (γ_2), dispersive (γ_{lv}^d) and polar (γ_{lv}^p) component values are detailed in Table 2. The experiments were conducted in atmospheric conditions at a temperature of 20°C. The droplets were released in a controlled manner onto the surface of the test substrate materials (laser treated and untreated) from the tip of a micropipette, with the resultant volume of the drops being approximately $6 \times 10^{-3} \text{ cm}^3$. Each experiment lasted for three minutes with profile photographs of the sessile drops being obtained every minute. The contact angles were then subsequently measured. A mean value was subsequently determined.

It was observed during the wetting experiments conducted with both the enamel and the control liquids that, throughout the period of the experiments, no discernible change in the magnitude of the contact angle was observed, indicating that thermodynamic equilibrium was established at the solid-liquid interface at the outset of the experiments. This is perhaps surprising when one considers the temperature effect on surface tension as described by Mayers [25]. However, results similar to those observed in this study have been described by Agathopoulos et al [26].

3. Effects of laser radiation on contact angle characteristics

Prior to laser treatment of the AOCG surface it was not possible to fire the enamel onto the surface of the AOCG. This was found to be due to the fact that the contact angle between the enamel and the untreated AOCG surface was measured as being 118° , consequently preventing the enamel from wetting the AOCG surface.

Under the experimental laser parameters, interaction with the CO₂ laser, the Nd:YAG laser and the HPDL beams resulted in the contact angle between the enamel and the AOCG reducing from 118° to 31° , 34° and 33° respectively. In contrast, interaction of the AOCG with excimer laser radiation effected an increase in the contact angle to 121° .

Similarly, as Table 3 shows, with all the control liquids used the AOCG experienced a significant reduction in contact angle as a result of interaction with the CO₂ laser, the Nd:YAG laser and the HPDL beams, whilst interaction with the excimer laser beam again resulted in an increase in the contact angle.

3.1. Variations in surface roughness characteristics

According to Neumann [27, 28], a model similar to that for heterogeneous solid surfaces can be developed in order to account for surface irregularities, being given by a rearrangement of Wenzel's equation:

$$\gamma_{sl} = \gamma_{sv} - \left(\frac{\gamma_{lv} \cos \theta_w}{r} \right) \quad (1)$$

where, r is the roughness factor defined as the ratio of the real and apparent surface areas and θ_w is the contact angle for the wetting of a rough surface. Equation (1) shows clearly that if the roughness factor, r , is large, that is the solid surface is smooth, then γ_{sl} will become small, thus, a reduction in the contact angle will be inherently realised by the liquid if $\theta < 90^\circ$. In contrast, if $\theta > 90^\circ$ then the opposite will be observed.

Indeed, considerable reductions in the surface roughness of the AOCG were observed after interaction with the CO₂ laser, the Nd:YAG laser and the HPDL beams, reducing from an initial Ra value of 25.85µm to 5.88µm, 6.56µm and 6.27µm respectively. In contrast, interaction of the AOCG with excimer laser radiation resulted in a roughening of the AOCG surface, causing the surface roughness to increase to an Ra value of 36.22µm.

The smoothing effects of CO₂ laser, Nd:YAG laser and HPDL irradiation on the surface of the AOCG in comparison with the roughening effects of excimer laser irradiation are clearly discernible from Figure 2.

3.2. Variations in surface oxygen content

The O₂ content of a material's surface is most certainly an influential factor effecting the wetting performance of the material [29, 30]. Wetting is governed by the first atomic layers of the surface of a material. Thus, in order to determine element content of O₂ at the surface of the AOCG, it was necessary to examine the surface using x-ray photoemission spectroscopy (XPS).

Significant differences in the surface O₂ content of the AOCG after interaction with all the selected lasers were observed. Increases in the surface O₂ content were experienced by the AOCG after interaction with CO₂ laser, the Nd:YAG laser and the HPDL beams, increasing from an initial value of 37.6at.% to 43.1at.%, 41.4at.% and 42.8at.% respectively. Conversely, interaction of the AOCG with excimer laser radiation resulted in the surface O₂ content of the AOCG decreasing slightly to 33.4at.%.

4. Surface energy and the dispersive/polar characteristics

The intermolecular attraction which is responsible for surface energy, γ , results from a variety of intermolecular forces whose contribution to the total surface energy is additive [31]. The majority of these forces are functions of the particular chemical nature of a certain material, and as such the total surface energy comprises of γ^p (polar or non-dispersive interaction) and γ^d (dispersive component; since van der Waals forces are present in all systems regardless of their chemical nature). Therefore, the surface energy of any system can be described by [31]

$$\gamma = \gamma^d + \gamma^p \quad (2)$$

Similarly, W_{ad} can be expressed as the sum of the different intermolecular forces that act at the interface [31]:

$$W_{ad} = W_{ad}^d + W_{ad}^p = 2(\gamma_{sv}^d \gamma_{lv}^d)^{1/2} + 2(\gamma_{sv}^p \gamma_{lv}^p)^{1/2} \quad (3)$$

By equating Equation (3) with the Young-Dupre Equation:

$$W_{ad} = \gamma_{lv}(1 + \cos \theta) \quad (4)$$

Then the contact angle for solid-liquid systems can be related to the surface energies of the respective liquid and solid by

$$\cos \theta = \frac{2(\gamma_{sv}^d \gamma_{lv}^d)^{1/2} + 2(\gamma_{sv}^p \gamma_{lv}^p)^{1/2}}{\gamma_{lv}} - 1 \quad (5)$$

In accordance with studies conducted by Fowkes [31] and Agathopoulos [26], it is possible to estimate reasonably accurately the dispersive component of the AOCG surface energy, γ_{sv}^d , by plotting the graph of $\cos \theta$ against $(\gamma_{lv}^d)^{1/2}/\gamma_{lv}$ in accordance with Equation (5) [31], with the value of γ_{sv}^d being estimated by the gradient ($=2(\gamma_{sv}^d)^{1/2}$) of the line which connects the origin ($\cos \theta = -1$) with the intercept point of the straight line ($\cos \theta$ against $(\gamma_{lv}^d)^{1/2}/\gamma_{lv}$) correlating the data point with the abscissa at $\cos \theta = 1$. Figure 3 shows the best-fit plot of $\cos \theta$ against $(\gamma_{lv}^d)^{1/2}/\gamma_{lv}$ for the untreated and laser treated AOCG-experimental control liquids system.

A comparison of the ordinate intercept points of the untreated and laser treated AOCG-liquid systems, shown in Figure 3, shows clearly that for the untreated and excimer laser treated AOCG-liquid systems, the best-fit straight line intercepts the ordinate relatively close to the

origin. In contrast, Figure 3 shows that the best-fit straight line for the AOCG-liquid systems of the CO₂, Nd:YAG and HPDL treated samples intercept the ordinate considerably higher above the origin. This is of great importance since interception of the ordinate close to the origin is characteristic of the dominance of dispersion forces acting at the AOCG-liquid interfaces of the untreated and excimer laser treated samples, resulting in poor adhesion [31, 32]. While an interception of the ordinate well above the origin is indicative of the action of polar forces across the interface, in addition to dispersion forces, hence improved wettability and adhesion is promoted [31, 32]. Furthermore, because none of the best-fit straight lines intercept below the origin, then it can be said that the development of an equilibrium film pressure of adsorbed vapour on the AOCG surface (untreated and laser treated) did not occur [31, 32].

Again, in accordance with studies conducted by Fowkes [31] and Agathopoulos [26], it is not possible to determine the value of the polar component of the AOCG surface energy, γ_{sv}^p , directly from Figure 3. This is because the intercept of the straight line ($\cos \theta$ against $(\gamma_{lv}^d)^{1/2}/\gamma_{lv}$) is at $2(\gamma_{sv}^p \gamma_{lv}^p)^{1/2}/\gamma_{lv}$, and thus only refers to individual control liquids and not the control liquid system as a whole. However, it has been established that the entire amount of the surface energies due to dispersion forces either of the solids or the liquids are active in the wettability performance [31, 33]. As such, it is possible to calculate the dispersive component of the work of adhesion, W_{ad}^d , using only the relevant part of equation (3) thus

$$W_{ad}^d = 2(\gamma_{sv}^d \gamma_{lv}^d)^{1/2} \quad (6)$$

The results reveal that for each particular control liquid in contact with both the untreated and laser treated AOCG surfaces, both W_{ad} and W_{ad}^d are related by the straight line relationship

$$W_{ad} = aW_{ad}^d + b \quad (7)$$

where a and b are constants unique to each control liquid system. Also, for the control test liquids used, a linear relationship between the dispersive and polar components of the control test liquids surface energies has been deduced which satisfies the equation

$$(\gamma_{lv}^p)^{1/2} = 1.3(\gamma_{lv}^d)^{1/2} + 1.15 \quad (8)$$

By introducing Equation (7) into Equation (3) and rearranging, then

$$W_{ad}^p = (a - 1)W_{ad}^d + b \quad (9)$$

By combining Equation (9) with Equation (3) and differentiating with respect to $(\gamma_{lv}^d)^{1/2}$, then the following can be derived:

$$(\gamma_{sv}^p)^{1/2} = \frac{(\gamma_{sv}^d)^{1/2} (a-1)}{1.3} \quad (10)$$

Thus, from the best-fit straight line plots of W_{ad} against W_{ad}^d for the AOCG when it is both untreated and laser treated, it is possible to determine the constants a and b for each separate condition of the AOCG, as shown in Table 4. Since γ_{sv}^d has already been determined for the untreated and laser treated AOCG from Figure 3, then it is possible to calculate γ_{sv}^p for untreated and laser treated AOCG using Equation (10).

As one can see from Table 5, CO₂ laser, Nd:YAG laser and HPDL treatment of the surface of the AOCG result in an overall increase in the total surface energy γ_{sv} , whilst significantly increasing also the polar component of the surface energy γ_{sv}^p . Such increases in the surface energy of the AOCG, in particular the increase in γ_{sv}^p , have a positive effect upon the action of wetting and adhesion. Again, these changes in the surface energy of the AOCG after treatment with these lasers is primarily due to the fact that the treatment of the AOCG surface results in the melting and partial vitrification of the surface; a transition that is known to effect an increase in γ_{sv}^p [26], consequently causing a decrease in the contact angle.

5. Discussion of laser effected wettability characteristics modification

The results detailed previously show clearly that interaction of the AOCG with selected industrial lasers has resulted in the contact angle formed between the enamel and the control liquids altering to various degrees depending upon the laser type. Under the selected experimental laser operating parameters, interaction of the AOCG typically with the CO₂ laser, the Nd:YAG laser and the HPDL beams resulted in decrease of similar proportion in the contact angle, whilst interaction of the AOCG with excimer laser radiation resulted in an increase in the contact angle. Such changes in the value of the contact angle are influenced, depending upon the laser used, primarily by:

1. *Surface Melting and Partial Vitrification* - Laser induced melting and vitrification results in the occurrence of two main changes in the surface condition of the AOCG. These are:

- i. *Surface Smoothing* resulting from the laser melting of the AOCG surface which consequently results in a reduction of the surface roughness, thus directly reducing the contact angle, θ .
 - ii. *Increase in the Polar Component, γ_{sv}^p , of the Surface Energy* resulting from the melting and partial laser vitrification of the glass forming elements within the AOCG composition, thus improving the action of wetting and adhesion by generating a surface with a more vitreous surface microstructure.
2. *Surface Roughening* - An increase in the AOCG surface roughness resulting from laser ablation of the AOCG surface in turn results directly in an increase in the contact angle, θ .
 3. *Surface O₂ Content* - An increase in the surface O₂ content of the AOCG resulting from laser treatment is an influential factor in the promotion of the action of wetting, since an increase in surface O₂ content inherently effects a decrease in the contact angle, and vice versa.

It is highly likely that the resultant contact angle between the AOCG-enamel and the AOCG-liquid systems of the CO₂, Nd:YAG and the HPDL treated samples are all similar in value due to the fact that interaction with these lasers caused surface melting (see Figure 2), resulting in a significantly smoother surface. This, combined with the fact that vitrification of the AOCG surface results in an increase in the polar component of the surface energy, γ_{sv}^p , as a result of the surface becoming less crystalline in nature, thus promoting wetting, would influence a reduction in the contact angle. From Table 5 it can be seen that interaction of the AOCG with CO₂, Nd:YAG and the HPDL radiation resulted in similar increases in γ_{sv}^p . However, absorption of CO₂ radiation by the AOCG is higher than that of the Nd:YAG or the HPDL [34], and, since contact angle reduction is a function of surface melting and vitrification [34], then surface melting and vitrification will occur to a greater extent with the CO₂ laser, thus resulting in a marginally greater decrease in the contact angle.

In contrast, as Figure 2(e) shows, interaction of the AOCG with excimer laser radiation did not cause melting of the surface, but instead induced surface ablation which consequently resulted in a slightly rougher surface. Thus an increase in the contact angle was effected. Additionally, Kokai et al [35] have concluded that, with excimer laser parameters which are conducive to the production of plasma, as was the case with the AOCG, then the surface roughness is increased as a result of plasma induced debris redepositing on the surface and excessive thermally induced surface fractures and porosities. Clearly, since plasma generation was observed, then surface roughening after excimer laser irradiation was perhaps to be expected. However, both

Liu et al [36] and Nicolas et al [37] have reported that irradiating ZrO₂ with excimer laser radiation with energy densities in excess of 2.7 J/cm², resulted in a reduction in surface roughness. Such reductions were attributed to the fact that at these levels of energy density, melting of the ZrO₂ surface occurred.

It was found that the depth of the laser melting, and in the case of the excimer laser, the ablation region, varied significantly according to laser type. Table 6 shows the differences in laser melt/ablation depth determined for each laser by means of cross-sectional SEM analysis. As Table 6 shows, the differences in laser melt/ablation depth obtained with the Nd:YAG and excimer lasers was an order of magnitude smaller than those of the CO₂ laser or HPDL. The main reason for these large differences are thought to be due to the pulsed nature of the beams of the Nd:YAG and excimer lasers, as opposed to the CW nature of the CO₂ laser or HPDL beams. Since the interaction time of a pulsed beam with a material is much shorter than that of a CW beam, then consequently the depth of the laser melt/ablation region will be much smaller due to the reduced time afforded for heat transfer.

It is also of great importance to consider the surface O₂ content of the AOCG before and after treatment with the selected lasers. Increases in the surface O₂ content were experienced by the AOCG after interaction with CO₂ laser, the Nd:YAG laser and the HPDL beams, whilst interaction of the AOCG with excimer laser radiation resulted in the surface O₂ content of the AOCG decreasing. Such a result is in agreement with the findings of a number of workers [38, 39], who have noted that for many ceramic materials, irradiation with an excimer laser beam creates defective energy levels, in particular the formation of O₂ vacancies.

Since roughening of the surface does not necessarily create a surface with a more crystalline structure, then it is reasonable to assume that the increase in the surface roughness after excimer laser irradiation, along with the associated reduction on the surface O₂ content, are the principal reasons for the observed decrease in the contact angle.

6. Conclusion

Interaction of CO₂, Nd:YAG, excimer and high power diode laser (HPDL) radiation with the surface of the AOCG was found to effect significant changes in the wettability characteristics of the material. It was observed that interaction with CO₂, Nd:YAG and HPDL radiation reduced the enamel contact angle from 118° to 31°, 34° and 33° respectively. In contrast, interaction with excimer laser radiation resulted an increase in the contact angle to 121°. Such changes were identified as being primarily due to: (i) the melting and partial vitrification of the AOCG surface as a result of interaction with CO₂, Nd:YAG HPDL radiation. This in turn generated a smoother surface and increased the polar component of the AOCG surface energy.

(ii) the surface roughness of the AOCCG increasing after interaction with excimer laser radiation due to ablation of the surface which in turn resulted directly in an increase in the contact angle.

(iii) the surface O₂ content of the AOCCG increasing after interaction with CO₂, Nd:YAG and HPDL radiation due to surface melting. Whilst conversely, the surface O₂ content of the AOCCG decreased after interaction with the excimer laser due to the creation of defective energy levels.

A wavelength dependence of the change of the wetting properties can not be deduced from the findings of this work. This is apparent from the very similar properties of the surfaces irradiated with the CO₂ laser, the Nd:YAG laser and the HPDL, the wavelengths of which vary by more than an order of magnitude. Nonetheless, the work has shown that under the chosen experimental laser operating parameters, changes in the wettability characteristics of the AOCCG were seen to vary depending upon the laser type. In particular, whether the laser radiation had the propensity to cause surface melting. Similar effects of laser surface treatment have been observed for other ceramic materials when treated with a HPDL [23].

References

1. Steg P G, Astier R, Englander J, Lavergne A and Lencarpen D 1986 *Archives des Maladies du Coeur des Vaisseaux* **4** 558
2. Miki T, Inoue K, Obana A and Shiraki K 1989 *Lasers in Surgery and Medicine* **9** 543-55
3. Schomaker K T, Domankevitz Y, Flotte T J and Deutsch T F 1991 *Lasers in Surgery and Medicine* **11** 141-47
4. Tassignon M J, Stempels N Nguyenlegros J and Dewilde F 1991 *Clinical and Experimental Ophthalmology* **229** 380-88
5. Canning C, Polkinhorne P, Ariffen A and Gregor Z 1991 *Brit. J. Ophthalmology* **75** 602-10
6. McMillan T A Stewart W C Nutaitis M J and Powers T P 1992 *Acta Ophthalmologica* **70** 758-61
7. Wyman D R Schatz S W and Maguire J A C 1997 *Lasers in Surgery and Medicine* **21** 50-8
8. Dausinger F 1990 *Proc. of ECLAT'90: Laser Treatment of Materials* Vol 1 1-14
9. Shuttleworth S 1996 *App. Surf. Sci.* **96-98** 513-17
10. Dyer P E, Gonzalo J, Key P E Sands D and Schmidt M J J 1997 *App. Surf. Sci.* **110** 345-49
11. Chen X, Lotshaw W T, Ortiz A L, Staver P R and Erikson C E 1996 *J. of Laser Apps.* **8** 233-39
12. Schmidt M J J, Li L and Spencer J T 1998 *App. Surf. Sci.* **138-139** 378-84
13. Bradley, L, Li L and Stott F H 1998 *App. Surf. Sci.* **138-139** 522-28
14. Lawrence J, Li L and Spencer J T 1996 *Proc. of ICALEO'96: Laser Materials Processing* Vol 81A 138-48
15. Lawrence J, Li L and Spencer J T 1998 *Optics & Laser Tech.* **30** 205-14
16. Lawrence J, Li L and Spencer J T 1998 *Optics & Laser Tech.* **30** 215-23
17. Zhou X B, De Hosson J Th M 1993 *J. de Physique IV* **3** 1007-11
18. Zhou X B, De Hosson J Th M 1994 *Acta Met. et Mat.*, **42** 1155-62
19. Bahnert T, Kesting W and Schollmeyer E 1993 *App. Surf. Sci.* **69** 12-15
20. Bahnert T 1993 *Optics & Quantum Elect.* **27** 1337-48

21. Heitz J, Arenholz E, Kefer T, Bäuerle D, Hibst H and Hagemeyer A 1992 *App. Phys. A* **55** 391-92
22. Olfert M, Duley W and North T 1996 *Laser Processing: Surface Treatment and Film Deposition* eds. J Mazumder, O Conde, R Villan and W M Steen (Amsterdam: Kluwer Academic Publishers) 479-90
23. Lawrence J, Li L and Spencer J T 1998 *App. Surf. Sci.* **138-139** 195-201
24. Gutowski V W, Russell L and Cerra A 1992 *Science and Technology of Building Seals, Sealants, Glazing and Waterproofing* ed. J M Klosowski (Philadelphia: ASTM) 144-59
25. Mayers D 1991 *Surfaces, Interfaces and Colloids* (Berlin: VCH Publishers) 142
26. Agathopoulos S and Nikolopoulos P 1995 *J. Biomed. Mat. Res.* **29** 421-29
27. Neumann A W and Good R J 1972 *J. Colloid and Interface Sci.* **38** 341-51
28. Neumann A W 1978 *Wetting Spreading and Adhesion* ed. J F Padday (London: Academic Press) 3-35
29. Ueki M, Naka M and Okamoto I 1986 *J. Mat. Sci. Lett.* **5** 1261-62
30. Li J G 1993 *Rare Metals* **12** 84-96
31. Fowkes F M 1964 *Ind. Eng. Chem.* **56** 40-52
32. Chattoraj D K and Birdi K S 1984 *Adsorption and the Gibbs Surface Excess* (New York: Plenum Press)
33. Good R J and Girifalco L A 1960 *J. Phys. Chem.* **64** 561-65
34. Lawrence J 1998 PhD Thesis, UMIST. *To be submitted*
35. Kokai F, Amano K, Ota H and Umemura F 1992 *App. Phys. A* **54** 340-42
36. Liu Z, Steen W M and O'Neill W 1990 *4th Int. Conf. On Surface Modification Technologies*
37. Nicolas G, Autric M, Marine W and Shafeev G A 1997 *App. Surf. Sci.* **109/110** 289-92
38. Filotti L, Bensalem A and Shafeev G A 1997 *App. Surf. Sci.* **110** 249-53
39. Shafeev G A and Sissakyn E V 1997 *Laser Phys.* **3** 110-20

List of Figures

Figure 1. Schematic of the set-up for the CO₂, Nd:YAG, HPDL and excimer laser interaction experiments with the AOCG.

Figure 2. Typical SEM surface images of the AOCG (a) before laser treatment and after laser interaction with (b) CO₂ laser, (c) Nd:YAG laser, (d) HPDL and (e) excimer laser radiation.

Figure 3. Plot of $\cos \theta$ against $\left(\gamma_{lv}^d\right)^{1/2} / \gamma_{lv}$ for the AOCG in contact with the wetting test control liquids, before and after laser treatment.

Figure 1

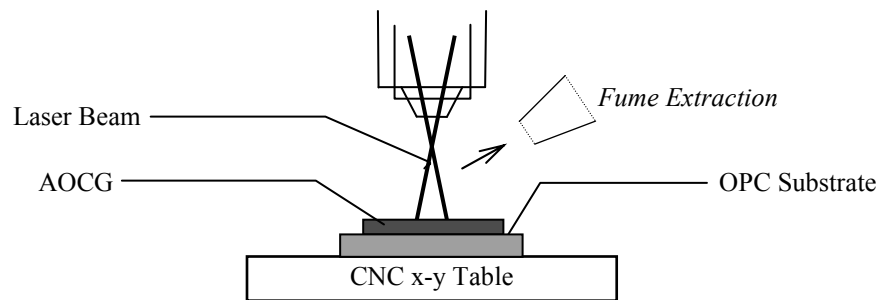
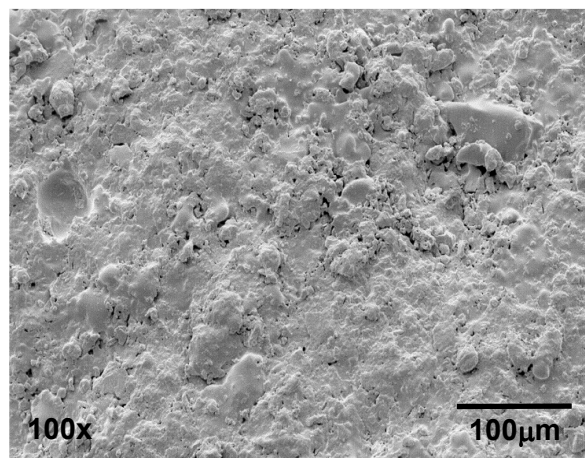
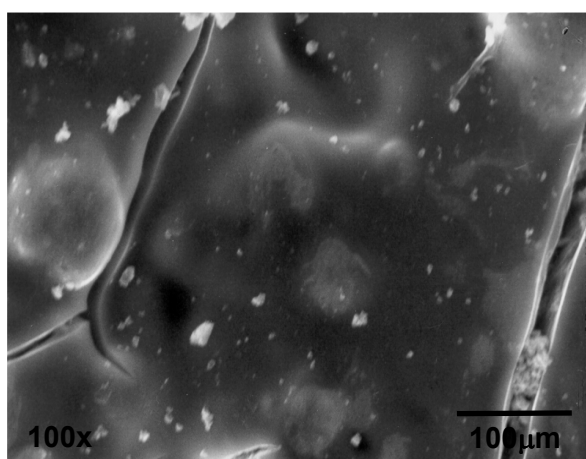


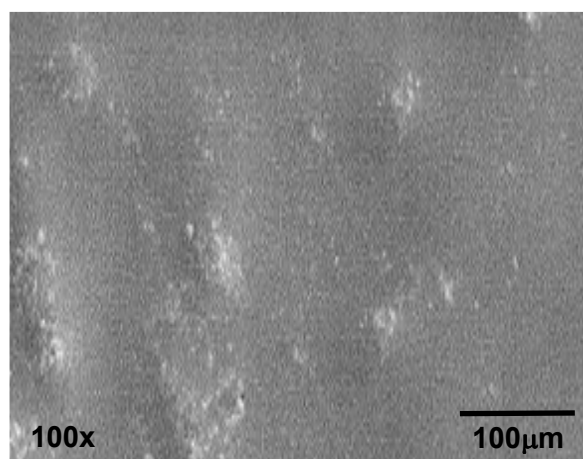
Figure 2



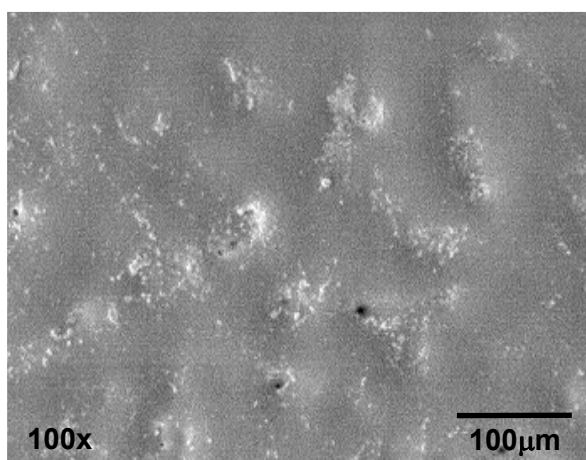
(a)



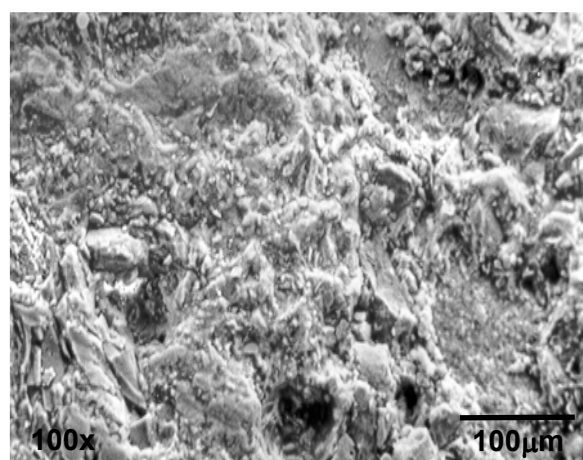
(b)



(c)

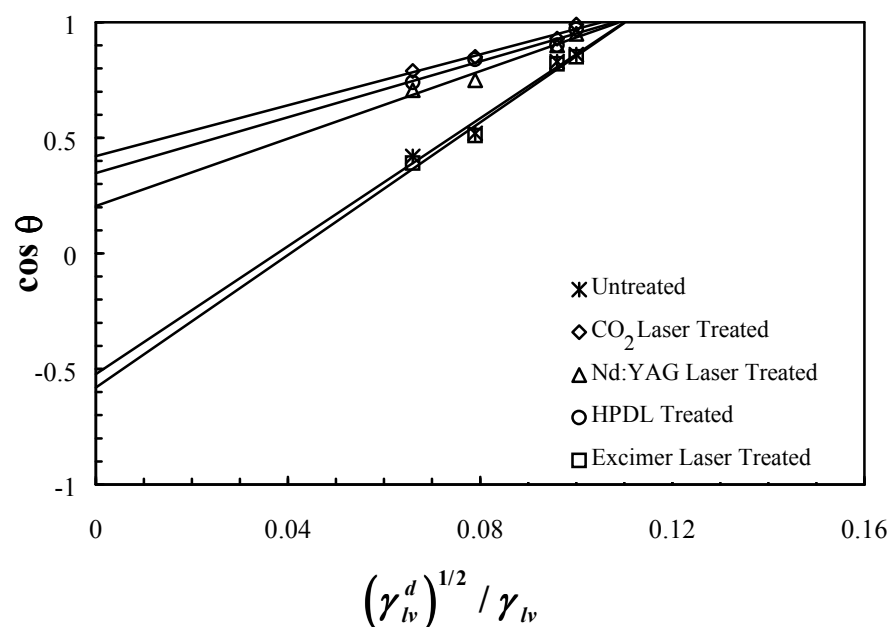


(d)



(e)

Figure 3



List of Tables

Table 1. Details of the selected industrial lasers used.

Table 2. Total surface energy (γ_{lv}) and the dispersive (γ_{lv}^d) and polar (γ_{lv}^p) components for the selected test liquids [24].

Table 3. Mean values of contact angles formed between the selected test liquids at 20°C and the AOCG before and after interaction with the selected lasers.

Table 4. Values determined for the constants a and b from the plots of W_{ad} against W_{ad}^d for the AOCG, before and after laser treatment.

Table 5. Determined surface energy values for the AOCG before and after laser irradiation.

Table 6. Determined laser melt/ablation depths for the AOCG after laser irradiation.

Table 1

Operating Characteristic	Laser			
	CO ₂	Nd:YAG	HPDL	Excimer
Lasant	CO ₂ gas	Nd:YAG crystal	GaAlAs	KrF gas
Wavelength	10.6µm	1.06µm	810 ±20nm	248nm
Maximum Average Output	1 kW	400 W	60 W	5 W
Maximum Pulse Energy	~	70 J	~	35 J
Pulse Width	~	0.3 - 10 ms	~	20 ns
Repetition Rate	~	1 - 1000 Hz	~	1-55 Hz
Fibre Core Diameter	~	600µm	600µm	~
Mode of Operation	CW	Pulsed (rapid)	CW	Pulsed (multiple)

Table 2

Liquid	γ (m Jm⁻²)	γ_{lv}^d (m Jm⁻²)	γ_{lv}^p (m Jm⁻²)
Human Blood	47.5	11.2	36.3
Human Blood Plasma	50.5	11.0	39.5
Glycerol	63.4	37.0	26.4
4-Octanol	27.5	7.4	20.1

Table 3

Liquid	Contact Angle, θ (deg)				
	Untreated	CO₂	Nd:YAG	HPDL	Excimer
Human Blood	61	34	38	37	74
Human Blood Plasma	64	35	39	38	84
Glycerol	34	27	29	28	57
4-Octanol	29	24	27	26	44

Table 4

AOCG Condition	a	b (mJ/m²)
Untreated	1.20	11.28
CO ₂ Laser	1.86	-17.08
Nd:YAG Laser	1.84	-21.47
HPDL	1.70	-18.27
Excimer Laser	1.08	13.21

Table 5

Surface Energy Component	AOCG Condition				
	Untreated	CO ₂	Nd:YAG	HPDL	Excimer
Dispersive Component, γ_{sv}^d	84.16	90.70	86.61	89.04	76.95
Polar Component, γ_{sv}^p (mJ/m ²)	2.00	36.83	36.16	25.87	0.29
Total, γ_{sv} (mJ/m ²)	86.16	127.53	122.77	114.91	77.24

Table 6

	Laser			
	CO₂	Nd:YAG	HPDL	Excimer
Laser Melt/Ablation Depth	210μm	50μm	125μm	30μm